ISA Transactions 53 (2014) 1650–1660

Contents lists available at ScienceDirect

ISA Transactions

journal homepage: www.elsevier.com/locate/isatrans

Bi-spectrum based-EMD applied to the non-stationary vibration signals for bearing faults diagnosis

Lotfi Saidi*, Jaouher Ben Ali, Farhat Fnaiech

University of Tunis, Tunis National Higher School of Engineering (ENSIT), Laboratory of Signal Image and Energy Mastery (SIME), 5 avenue Taha Hussein, PO Box 56, 1008 Tunis, Tunisia

ARTICLE INFO

Article history:
Received 2 March 2014
Received in revised form
23 May 2014
Accepted 5 June 2014
Available online 26 June 2014
This paper was recommended for publication by Dr. Jeff Pieper.

Keywords:
Bi-spectrum
Empirical mode decomposition
Fault diagnosis
Induction motor
Intrinsic mode function
Rolling element bearing

ABSTRACT

Empirical mode decomposition (EMD) has been widely applied to analyze vibration signals behavior for bearing failures detection. Vibration signals are almost always non-stationary since bearings are inherently dynamic (e.g., speed and load condition change over time). By using EMD, the complicated non-stationary vibration signal is decomposed into a number of stationary intrinsic mode functions (IMFs) based on the local characteristic time scale of the signal. Bi-spectrum, a third-order statistic, helps to identify phase coupling effects, the bi-spectrum is theoretically zero for Gaussian noise and it is flat for non-Gaussian white noise, consequently the bi-spectrum analysis is insensitive to random noise, which are useful for detecting faults in induction machines. Utilizing the advantages of EMD and bi-spectrum, this article proposes a joint method for detecting such faults, called bi-spectrum based EMD (BSEMD). First, original vibration signals collected from accelerometers are decomposed by EMD and a set of IMFs is produced. Then, the IMF signals are analyzed via bi-spectrum to detect outer race bearing defects. The procedure is illustrated with the experimental bearing vibration data. The experimental results show that BSEMD techniques can effectively diagnosis bearing failures.

1. Introduction

Condition monitoring and fault diagnosis of rolling element bearings (REBs) timely and accurately is very important to ensure the reliability of rotating machinery. The mechanical vibration signal remains the most immediate, simple, and rich source of information for understanding phenomena related to bearing defects (BDs) [1]. It is certainly a source of basic and interesting information to be extracted using specific and appropriate techniques.

Over past few years, various signal analysis methods have been proposed to detect and diagnose BDs. These methods may be roughly classified into vibration and acoustic measurements, temperature measurements and wear debris analysis [2]. Among the schemes mentioned above, vibration measurements are the popular method, because vibration signals are directly associated with the structural dynamics of the machine being monitored [3]. When a fault occurs on one surface of a bearing, the vibration signal is characterized by the presence of periodic repetitive sharp peaks and further modulated by a number of harmonic frequencies [4]. However, the interesting information is often contained in the periodicity of the impacts, rather than in the rest of the signal frequency content. So an effective signal processing method is desired to provide more evident information for fault diagnosis of REBs.

Vibration signals acquired from bearings can be either stationary or non-stationary. While stationary signals are characterized by time-invariant statistical properties, such as the mean value, statistical properties of a non-stationary signal change over time [5,6]. Vibration signals from real-world bearings are almost always non-stationary since bearings are inherently dynamic (e.g., speed and load condition change over time). However, non-stationary signals are often approximated as stationary, especially within a short time window, time-frequency techniques wavelet analysis, and EMD.

Despite the inadequate second-order features, useful third-order information could be preserved in the signal, governed by non-linear phenomena. Bi-spectrum is an alternative method that can be typically used. Higher order statistics (HOS) have proved to have more diagnostic information. Advantages for using HOS include additive Gaussian noise suppression, non-minimum phase system identification, nonlinear system detection and identification [10,11].

Relatively, some literatures traiting the bi-spectrum diagnosis of BDs have been published, in [12] the twice slice of cyclic bi-spectrum (CBS) is used for the detection of BDs. This method

* Corresponding author. Tel.: +216 22169567; fax: (+216) 71391166.
E-mail address: lotfi.saidi@esstt.rnu.tn (L. Saidi).

http://dx.doi.org/10.1016/j.isatra.2014.06.002
0019-0578/

inherits the advantage of the CBS, and is not sensitive to noise. In addition, twice slice of CBS is more direct and clear to show the features for diagnosis purpose.

Saidi et al. [2,13] presented two HOS techniques, namely the power spectrum and the slices of bi-spectrum used for the analysis of induction machine stator current leading to the detection of electrical failures. Experimental signals have been analyzed highlighting that bi-spectrum results show their superiority in the accurate detection of rotor broken bars.

In [14], in order to process the non-stationary transient gearbox vibration signals effectively, the order bi-spectrum technique is presented. This method combines computed order tracking technique with bi-spectrum analysis. The order bi-spectrum method assists in spectral smearing and modulation effects cancellation caused by the shaft speed variation.

All these works, suppose the vibration signals as being stationary. To deal with the signals accurately, the present work proposes to analyze the BD's sensed signals by using EMD in order to decompose the signal in many IMFs stationary signals.

In this paper, we propose a combined method to detect BDs using EMD and bi-spectrum analysis, which is called bi-spectrum based-EMD (BSEMD), with attempts to identify the characteristics of BD. EMD is a fundamentally new approach to the decomposition of nonlinear and non-stationary signal presented originally by Huang et al. in 1988 [14]. EMD can decompose multi-component signals into a series of Intrinsic Mode Functions (IMFs) that are stationary. Thus, it is a self-adaptive signal processing technique that is suitable for nonlinear and non-stationary processes. Since EMD was introduced in 1998, it has been widely used in various applications, such as, process control [15], modeling [16], condition monitoring [17], etc.

Many researchers have applied EMD combining with other techniques to BDs diagnosis in recent years and achieved better diagnosis results compared with the use of EMD alone. Miao et al. [18] introduced a joint method based on EMD and independent component analysis for fault signature detection of bearing outer and inner race faults. Yu et al. [19] applied EMD and Hilbert transform to the envelope signals of bearings and produced the local Hilbert marginal spectrum to diagnose BDs. Li and Zheng [20] proposed a signal analysis approach based on EMD and Teager Kaiser energy operator for BD detection. Rai and Mohanty [21] introduced Fourier transform of IMFs into the Hilbert–Huang transform for discovering REB defects. Li et al. [22] applied Wigner–Ville distribution based on EMD to BD diagnosis and therefore prevented the presence of cross terms. Chen et al. [23] using EMD and Hilbert transform to generate the local marginal spectrum from which the outer and inner races BDs were diagnosed under transient conditions. Since, many studies have exploited the IMF of vibration signals from rotating machinery for condition monitoring and fault detection. However, most of the approach has been focused on analyzing the characteristics of individual IMF to extract fault-sensitive features.

The main problem in industrial application of bearing vibration diagnostics is the masking of useful information by the strong noise. The vibration signal of the rolling bearing is often concealed by other structural vibrations sources, such as gears. Although a number of vibration diagnostic techniques have been developed over the last several years, in many situations these methods are relatively complicated in use or only effective at later stages of damage development. This paper presents an EMD-based rolling bearing diagnosing method applied to the raw vibration signals that shows potential for bearing damage detection at a much earlier stage of damage development.

This paper is organized as follows: In Section 2, background on REB signals is introduced. In Section 3, both the methodology proposed to detect and diagnose faults in bearings and the description of the techniques involved in the main steps of the method are presented. In Section 4, the proposed method is validated using experimental bearing data. Finally, the conclusions of this work are given in Section 5.

2. Nonstationary nature of defective REBs vibration response

As shown in Fig. 1, a REB has four major components, outer race, inner racer, rolling elements, and cage. All four components might be damaged during operation. Generally, the signature of a damaged bearing consists of exponentially decaying ringing that occurs periodically at the characteristic frequency. The vibration signal of a defective bearing usually considers being amplitude modulated at characteristic defect frequency [3–6].

2.1. Bearing defects (BDs) signatures

Failure surveys [1,2] by the Electric Power Research Institute (EPRI) indicate that IMs bearing-related faults are about 40% among the most frequent faults in IMs [1–3]. As shown in Fig. 1, the bearings consist mainly of the outer and inner raceways, the balls, and the cage. BDs can be classified into two classes: single-point defects and generalized roughness. Single-point defects are localized and classified into:

- Outer raceway defect.
- Inner raceway defect.
- Ball defect.

Generalized roughness is a type of fault where the condition of a bearing surface has degraded considerably over a large area and become rough, irregular, or deformed.

These faults may enhance vibration and noise level [12]. Moreover, there are internal operating stresses caused by vibration, eccentricity, and bearing current. Additionally, bearings can also be affected by other external causes such as:

- Contamination and corrosion.
- Lack of lubrication causing heating and abrasion.
- Defect of bearing's mounting, by improperly forcing the bearing onto the shaft or in the IM's stand.

The single-point defect may be seen by fault frequencies appearing in the machine vibration spectrum record. The frequencies at which these components occur are predictable and depend on the surface on which the bearing contains the fault. Therefore,

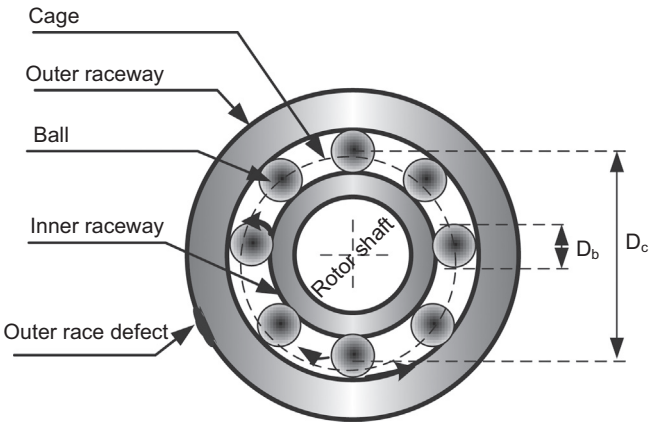

Fig. 1. REB geometry with damaged outer race.

there are different fault frequency characteristics associated with each component among the four parts of the bearing [12].

Rollers or balls rolling over a local fault in the bearing produce a series of force impacts. If the rotational speed of the races is constant, the repetition rate of the impacts is determined solely by the geometry of the bearing. The repetition rates are denoted bearing frequencies, for example, Ball Passing Frequency Outer Race (BPFO), Ball Passing Frequency Inner Race (BPFI), and Ball Fault Frequency (BFF) are frequently used. Their mathematical equations are as follows [12]:

$$BPFO = \frac{f_r}{2} N_b \left(1 - \frac{D_b}{D_c} \cos\ \theta\right) \quad (1)$$

$$BPFI = \frac{f_r}{2} N_b \left(1 + \frac{D_b}{D_c} \cos\ \theta\right) \quad (2)$$

$$BFF = \frac{f_r D_c}{2 D_b}\left[1 - \left(\frac{D_b}{D_c} \cos\ \theta\right)^2\right] \quad (3)$$

where f_r is the rotor shaft frequency, N_b is the number of rolling element, D_b is the ball diameter, D_c is the pitch diameter between two opposite rolling elements, and θ is the ball contact angle, angle of the load from the radial plane.

Table 1 shows the parameters of the bearing used in our experimental test bench (Figs. 7 and 8), taken from the data sheet [24].

Table 1
Drive end bearing information.

Bearing	SKF-6205
Geometry size [mm]	
Outside diameter	51.81
Inside diameter	2.49
N	9
D_c	201.9
D_b	38.86
$\cos\theta$	0.9
Defect frequencies multiple of running speed [Hz]	
Inner ring	5.4152
Outer ring	3.5848
Cage train	0.3983
Rolling element	4.7135

2.2. The characteristics of rolling bearing signals

A large number of models have been used to describe the dynamic behavior of rolling element bearings under different types of defects. According to the traditional approach [3], when rolling elements of bearing pass the defect location, wide band impulses are generated. And those impulses will then excite some of the vibrational modes of the bearing and its supporting structure. The excitation will result in the sensed vibration signals (waveforms) different in either the overall vibration level or the vibration magnitude distribution.

Measured vibration signals consist of two parts: $y(t)=v(t)+n(t)$, where $v(t)$ is the defect-induced impulse responses and $n(t)$ is the background noise, including vibration signals generated by other components, such as rotor unbalance and gear meshing. Because of the structure and the mode of operation of REBs, $v(t)$ has distinct features as follows [6,12]:

- Wide frequency range: BDs usually start as small pits or spalls, and give sharp impulses in the early stages covering a very wide frequency range.
- Small energy: The energy created by the BD is very small. A band has to be found where the bearing signal dominates over other components.
- Non-stationary signal: Incipient BDs produce a series of repetitive short transient forces, which in turn excite structural resonances.

Because the vibration signals generated by a defective REB have the characteristics mentioned above, it is difficult to identify their faults through a simple classical frequency analysis.

2.3. REB signals model

In this paper, the effectiveness of EMD-bispectrum method is illustrated on a synthetic signal of a REB with an outer race fault (ORF). This type of fault was chosen because it is relatively simple phenomenon to simulate while being often found in rotor machinery condition monitoring. REB with ORF during operation generates a series of periodic shock-pulses whose repetition rate depends on its dimensions and rotational speed of the shaft with which the bearing is assembled. Shock-pulses are generated each

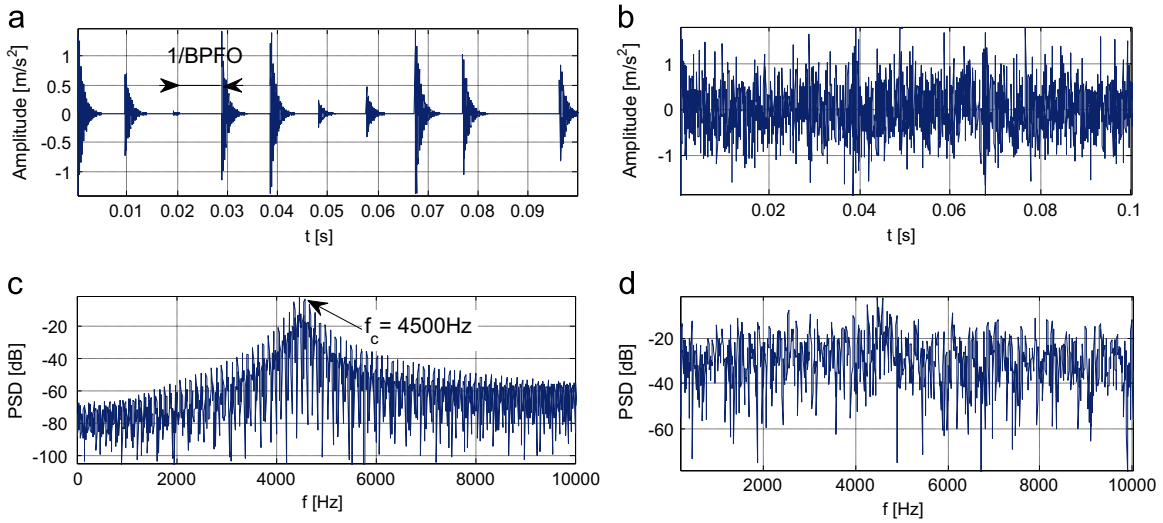

Fig. 2. Simulated short segment of vibration response data showing outer race impacts with (a) and without (b) noise effect, (a) and (b) Waveforms, (c) and (d) their power spectral densities (PSD) respectively.

time rolling elements strike the defected surface of the bearing outer race and consequently, excite resonances of the structure between the fault location and the vibration sensor [3]. The frequency of shock occurrence is usually called the ball pass frequency of the outer race (BPFO) and is given in Eq. (2).

Assuming constant rotational speed and load of the bearing, the vibration signals generated by a REB with defected outer race were modeled by Randall et al. as [3,6]:

$$v(t)=\sum_i \omega\left(t-i\frac{1}{BPFO}-\tau_i\right)+n(t), \tag{4}$$

where $\omega(t)$ is the waveform generated by a single impact (related to resonance frequencies of the system), τ_i is an independent and identically distributed random variable and $n(t)$ is an additive background random noise. It now has to be stated that τ_i introduces influence of the rolling elements slips into the model.

In order to exhibit the effect of the stochastic non-stationary nature of certain critical parameters like slip, on the vibration spectra, a typical example is considered. The simulated signal generated by Eq. (4), corresponds to the typical response of a bearing with an ORF. The shaft rotation speed f_r is 29.16 Hz, [f_r=rpm/60]. The characteristic bearing defect frequency BPFO is equal to 3.58 times the shaft rotation speed, leading to an estimation of the BPFO around 104 Hz. The excited natural frequency f_c of the system is assumed to be equal to 4500 Hz, which corresponds to the largest peak in the spectrum. The signal consists of 2048 samples and the sampling rate is equal to 20 KHz. Fig. 2 illustrates the waveform and spectra of the simulated signals with and without additive Gaussian white noise (AGWN) effect. In perfect agreement to the expected results of the model defined in Eq. (4), it can be found that a serious of spike pulses appear in the time domain waveforms, the interval of the spike pulses of the defect-induced impulses (1/BPFO=9.6 ms). Their amplitudes are maximum in the frequency band around the resonance frequency of 4500 Hz.

As seen on the spectrum in Fig. 2(d), no distinct spectral lines can be recognized. Information that could be obtained by examination of the spectrum is only the frequency characteristic of band-pass stationary Gaussian noise used in generated signal. For rotor-machinery vibration signals, natural resonances of the object usually manifest themselves in the same manner. However, for vibration-based condition monitoring purposes, information about high-frequency resonances have relatively limited value. We focus our interest on the phenomena that causes excitation of observed resonances. Due to this fact, the usage of an advanced statistical procedure is necessary.

Table 2
Energy percentage of IMF components.

Vibration signals	*Energy percentage*				
	P_1	P_2	P_3	P_4	P_5
HB	0.51529	0.26738	0.19391	0.029383	0.00945
ORF	0.71153	0.18232	0.14309	0.0334	0.01238

3. Brief description of empirical mode decomposition and bi-spectrum

3.1. Empirical mode decomposition (EMD)

EMD has been shown to be adaptable in applications where the signal is non-stationary [7,8]. A recent review of EMD applications in fault diagnosis of rotating machinery can be found in [8]. The authors presented the details of EMD in various applications, e.g. bearings, gears, rotors, etc. The authors also reviewed existing EMD methodologies and classified it into three different groups namely: (1) original EMD method alone, (2) improved EMD methods, and (3) combinations of EMD with other methods such as artificial neural network and support vector machine. In this paper, original EMD [8] is used for non-stationary vibration bearing data. The main function of EMD is to decompose the original vibration signal into several signals which has specific frequency called intrinsic mode functions (IMFs) based on the enveloping technique. The results of IMFs are from high frequencies to low frequencies. In condition monitoring of rolling bearing, EMD is used to reveal the frequency content of vibration signal by decomposing the original signal into several IMFs in order to determine whether the bearing signal has specific frequency content corresponds to the BD frequencies or not. The selected IMF is chosen when the decomposed frequencies are identical to one of the bearing fault frequencies (for example as shown in

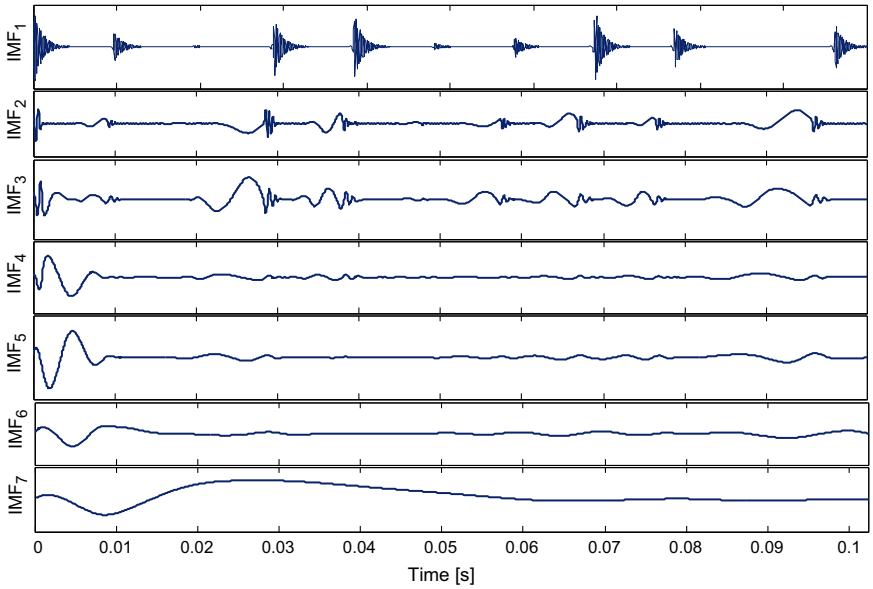

Fig. 3. IMF decomposition results of simulated vibration signal without noise, calculated by EMD.

Table 2) [8]. Fig. 3 shows the first eight IMF components decomposition of the vibration signal generated by Eq. (4), due to space limitation.

The multi-components signal (the current v in our case) is then decomposed into M intrinsic modes and a residue r [8].

$$v(t) = \Sigma_{i=1}^{M} IMF_i(t) + r(t) \tag{5}$$

IMFs are oscillatory signals that are locally zero-mean [8]. The residual $r(t)$ is the low-frequency mean trend. Note that all IMFs, except $r(t)$, are mean stationary. The higher order IMF index, i.e., M, is found by the algorithm itself and is signal-dependent. In this paper, the standard implementation proposed by Flandrin et al. [9] was used.

The effective algorithm for extracting the IMFs from a signal can be summarized as follows:

Step1 : *$r_0(t)=v(t)$ (the residual), $i=1$ (index number of IMF)*
Step1 : *extract the i-th IMF:*
- a- *Initialize: $h_o(t)=r_{i-1}(t)$; $j=1$ (index number of the iteration);*
- b- *Extract the local extrema of $h_{j-1}(t)$;*
- c- *Interpolate the local maxima and the local minima by cubic splines to form upper and lower envelope $e_{max}(t)$ and $e_{min}(t)$ respectively of $b_{j-1}(t)$;*
- d- *Calculate the mean of the upper and lower envelops: $m_{j-1}(t)=(e_{min}(t)+e_{max}(t)/2)$;*
- e- *If $b_j(t)$is a IMF then set $c_i(t)=b_j(t)$ else go to (b) with $j=j+1$;*

Step3 : *Update residual $r_i(t)=r_{i-1}(t)-c_i(t)$;*
Step4 : *If $r_i(t)$ still has at least two extrema then go to step2, with $i=i+1$ else the decomposition is finished and $r_i(t)$ is the residue.*

In addition, the implementation of EMD is a data-driven process, not requiring any pre-knowledge of the signal or the machine [8]. This particular advantage in electrical machines and drives context leads the EMD to be a promising tool to improve condition monitoring [8]. The EMD method has however several drawbacks. Choice of a relevant stopping criterion and mode-mixing problem are the most important topics that need to be addressed in order to improve the EMD algorithm [9].

We limit our effort to vibration signal only for the first seven IMFs. The IMFs extracted from vibration signal IMF_1 is associated with the local highest frequency and IMF_7 with the lowest frequency. In this paper the component in high frequency band (IMF_1) which represents the resonance modulation (about 4500 Hz) is selected for calculation.

The proposed methodology of our BSEMD diagnostic scheme is presented in Fig. 4 and discussed thoroughly the paper.

3.2. Bi-spectrum

The bi-spectrum belongs to the class of HOS, used to represent the frequency content of a signal. HOS provides higher order moments and nonlinear combinations of the higher order moments called cumulants [10,11]. Thus, HOS consist of moment and cumulant spectra. An overview of the theory on HOS can be found in [10,11]. Bi-spectral techniques show its effectiveness in quadratic phase coupling peak detection, and because it is a third order moment function, Gaussian background noise is eliminated in the estimation procedure [10].

The bi-spectrum can be estimated directly from the discrete Fourier transform of M realization of sampled version of the non-Gaussian third-order stationary and ergodic vibration signal $x(t)$ as follows:

$$\hat{B}(f_1,f_2) = \frac{1}{M}\sum_{i=1}^{M} X_i(f_1)X_i(f_2)X_i^*(f_1+f_2)$$
$$\approx E\{X(f_1)X(f_2)X^*(f_1+f_2)\} \tag{6}$$

where f_1, f_2 are the frequency indices, X^* denotes the complex conjugate of X and $X(f)$ is the Fourier transform of the discrete signal $x(n)$ and $E\{.\}$ is an average over an ensemble of realizations of a random signal. For deterministic signals, the relationship holds without an expectation operation with the third order correlation being a time-average [10,11].

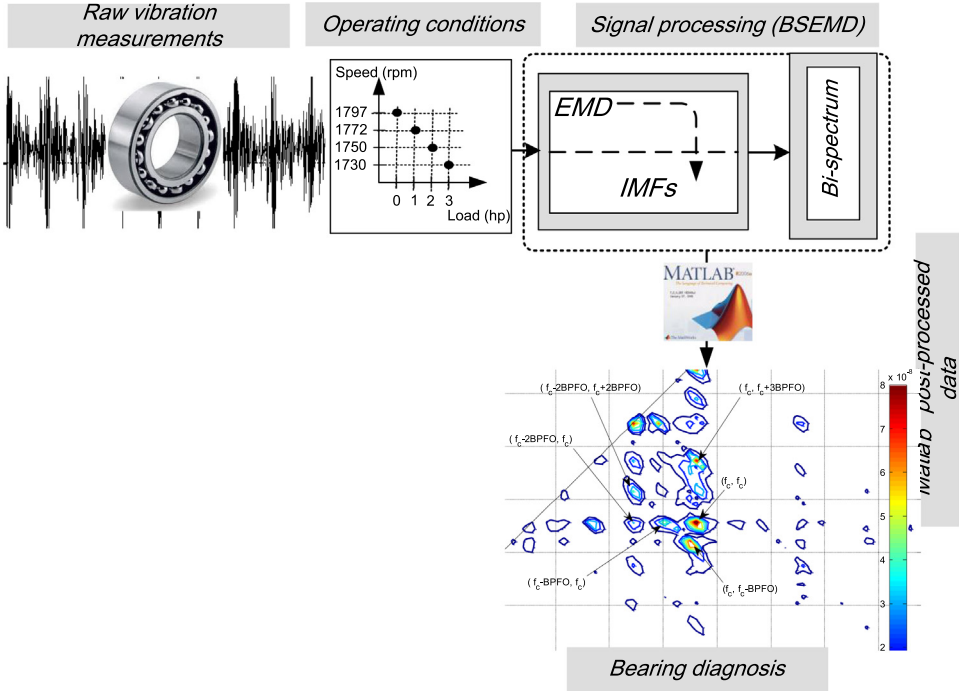

Fig. 4. Flowchart of the proposed diagnostic methodology for BDs.

The bi-spectrum of real signals contains a lot of symmetries and therefore redundant information. Redundant information already exists in the discrete Fourier transform. Despite these symmetries, here, all the information is displayed. However, focus is concentrated on the positive frequencies and of course only on the principal domain $\Im$ given by [10]:

$$\Im = \{(f_1, f_2) : 0 \le f_2 \le f_1 \le f_e/2, f_2 \le -2f_1 + f_e\} \quad (7)$$

where f_e is the sampling frequency.

In order to minimize the computational cost, the direct method [10,11] has been used to estimate and derived bi-spectrum features from vibration signals.

The BSEMD applied to the first IMF of simulated vibration ORF is shown in Fig. 5, and its enlarged presentation is shown in Fig. 6. The space between the peaks in the resonant frequency band is about 104 Hz, which is equal to the BPFO. In higher frequency band, the peaks around the highest peak are (f_c, f_c), $(f_c \pm \text{BPFO}, f_c)$.

The BSEMD based method combines the EMD and the bi-spectrum of the defective bearing non-stationary vibration signal. On the other hand, BSEMD can detect sets of frequency components that are phase-coupled.

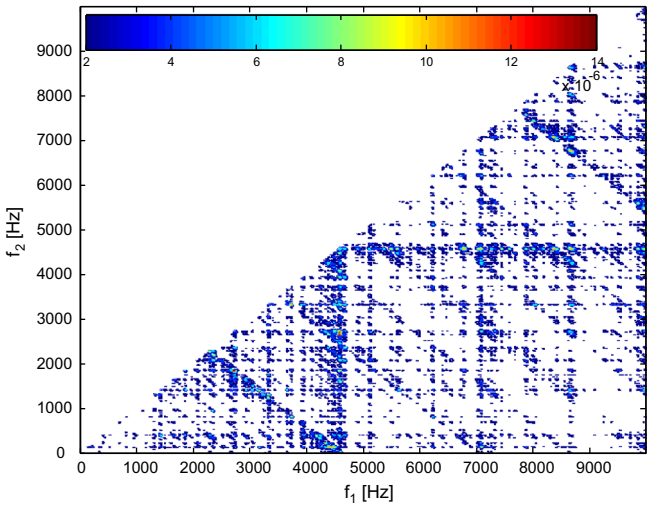

Fig. 5. BSEMD of simulated outer raceway vibration signal, result obtained by applying BSEMD to IMF_1.

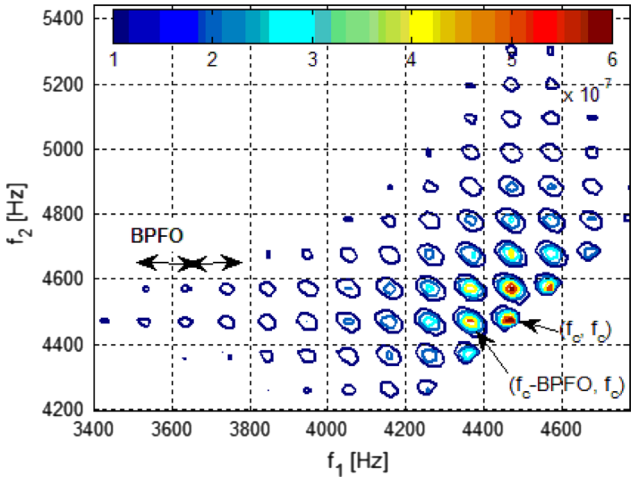

Fig. 6. Enlarged BSEMD of simulated outer raceway vibration signal in the bandwidth frequency between 3400 Hz and 4800 Hz, result obtained by applying BSEMD to IMF_1.

3.3. Stationarity test

Before applying power spectrum and bi-spectrum, signals must be stationary. Various methods exist for testing whether a given measurement signal may be regarded as a sample sequence of a stationary random sequence. A simple yet effective way to test for stationarity is to divide the signal into several (at least two) non-overlapping segments and then test for equivalency (or compatibility) of certain statistical properties (mean, mean-square value, power spectrum, etc.) computed from these segments. More sophisticated tests that do not require a priori segmentation of the signal are also available in [25,26].

The 3rd and 4th order cumulants of a discrete process $x(n)$ are expressed as follows [10,11]:

$$Cum_3(x) = E[x^3] - 3E[x]E[x^2] + 2E^3[x] \quad (8)$$

$$Cum_4(x) = E[x^4] - 4E[x]E[x^3] - 3E^2[x^2] + 12E^2[x][x^2] - 6E^4[x] \quad (9)$$

Let us calculate the 3rd and 4th order cumulants of the ORF vibration signal using Eqs. (8) and (9). The obtained values for the two cumulants are differents ($Cum_3 = 8.6736 \times 10^{-6}$, $Cum_4 = -6.5052 \times 10^{-8}$), so the non-stationarity hypothesis on ORF vibration is reinforced.

4. Experimental results

In this section, the BSEMD approach described above is applied to fault diagnosis of ORF-BDs.

4.1. CWRU bearing data: description of experimental set-up and data acquisition

The vibration data of roller bearings analyzed in this paper comes from Case Western Reserve University (CWRU) bearing data center. The detailed description about the test rig can be found in [24]. As shown in Figs. 7 and 8, the test rig consists of a 2 hp, three-phase induction motor (left), a torque transducer (middle), and a dynamometer-load (right). The transducer is used to collect speed and horsepower data. The load is controlled so that the desired torque load levels could be achieved. The test bearing supports the motor shaft at the drive end. Single point faults with fault diameters of 0.1778 mm, 0.3556 mm, and 0.5334 mm respectively, were introduced into the test bearing using electro-discharge machining. Vibration data are collected using an acquisition system at a sampling frequency of 12 kHz for different bearing conditions. The data recorder is equipped with low-pass filters at the input stage to avoid anti-aliasing. The geometry and defect frequencies of the two type bearings are listed in Table 1. Tests are carried out

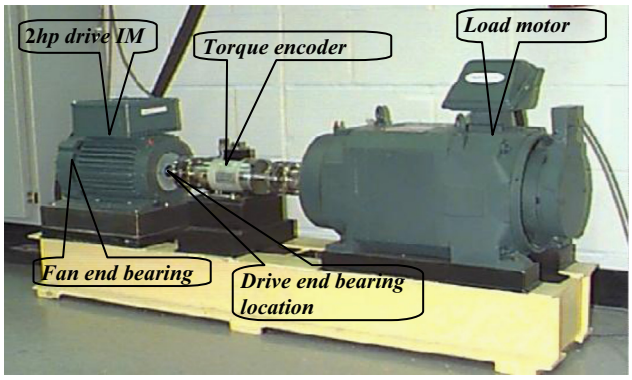

Fig. 7. Photo of the experimental test rig from CWRU, composed of a 2 hp motor (left), a torque transducer/encoder (center), load (right). The test bearings support the motor shaft [24].

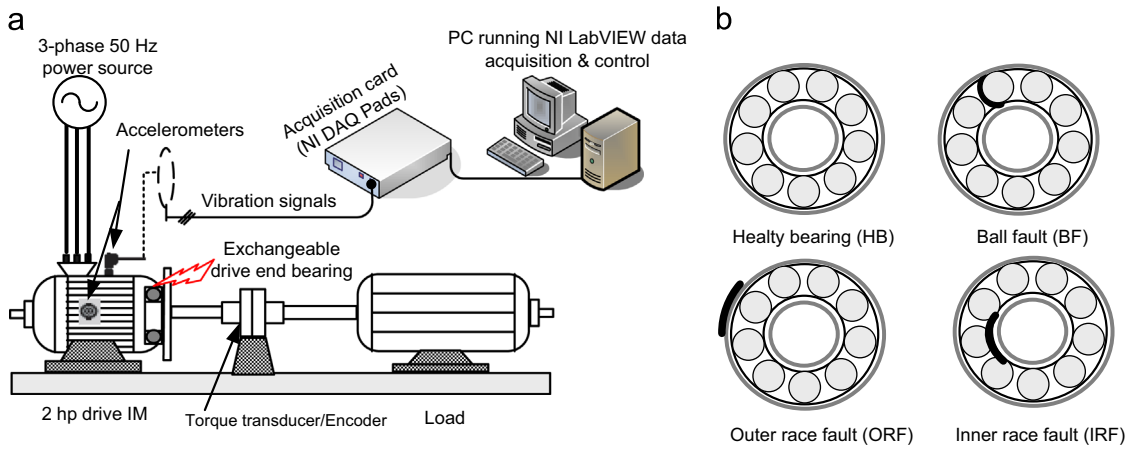

Fig. 8. (a) Schematic of the experimental test rig composed of a 2 hp motor (left), a torque transducer/encoder (center), load (right), and control electronics. The test bearings support the motor shaft. (b) A series of bearing components with faults induced in them indicated in bold line.

Table 3
Description of bearing data set analyzed under rated conditions.

Bearing condition		Fault specifications	
		Diameter [mm]	Depth [mm]
HB	HB	0	0
IRF	IRF_{17}	0.1778	0.279
	IRF_{35}	0.3556	0.279
	IRF_{53}	0.5334	0.279
	IRF_{71}	0.7112	0.279
BF	BF_{17}	0.1778	0.279
	BF_{35}	0.3556	0.279
	BF_{53}	0.5334	0.279
	BF_{71}	0.7112	0.279
ORF	ORF_{17}	0.1778	0.279
	ORF_{71}	0.7112	0.279
	ORF_{53}	0.5334	0.279

under different loads varying from 0 hp to 3 hp with 1 hp increments. The corresponding speed varies from 1797 rpm to 1730 rpm. BDs cover inner and outer races, and ball faults. The deep groove ball bearing 6205-2RS JEM SKF is used in the tests. Single point defects were set on the test bearings separately at the rolling element, inner raceway and outer raceway using electro-discharge machining. Accelerometers were placed at the 12 o'clock position when the defects were at the rolling element and inner raceway, and at the 6 o'clock position for the outer raceway defect. The parameters on the signals to be analyzed are listed in Table 3. More detailed information about the test-rig can be found in [24].

4.2. Analysis of the results

Although larger FFT bins produce a bi-spectrum with higher resolution, the computational load will also increase significantly. As a trade-off between resolution and computational expense, we set the FFT bin size as 1024. Moreover, it is recommended that the number of averaged segments shall exceed the number of the samples per segment [6–8]. So each segment with the size of 1024 samples was employed to calculate segment bi-spectrum, and then the final bi-spectrum was achieved by average bi-spectrum of 118 segments.

The time domain vibration signals of different bearing conditions under the same operating condition (1750 rpm speed and 1 hp load) are presented in Fig. 9.

As it is shown in Fig. 3, the different bearings conditions exhibit different vibration signal characteristics, such as signal variation ratio from the mean, magnitude and others.

For the healthy and outer raceway defective bearing signals, the raw signals and their power spectral densities (PSDs) are shown in Fig. 10(b) and (d), where the structural defect-induced impulses cannot be seen from the waveform due to the heavy background noise interference. The central frequency f_c is equal to 3480 Hz, is got from the highest spectral line in Fig. 10(d). Nevertheless, the fault signature is still hardly found in the power spectrum. Moreover, it can be seen from the power spectrum in Fig. 10(d), though the defect-induced frequency, the noise components around BPFO have higher power than it, which may make the diagnosis result be hardly convinced.

From Figs. 11 and 12, we can see the EMD method is acting as a set of filters and has decomposed the original vibration signal into eight bands from high to low frequency.

As shown in Fig. 13, the bi-spectrum contour plot is dominated by the presence of a number of distinct peaks around the central frequency f_c. For better resolution, this part of the picture is enlarged in Fig. 14. Characteristic peaks around the central frequency pair (f_c, f_c) can be clearly observed. The peak distances are equal to the sums and the differences between the central frequency f_c, the bearing defect frequency BPFO and its sub-harmonic multiple exactly at $2\times$BPFO. The presence of these peaks, which are associated with the harmonic of the BPFO, requires particular attention, since it provides a further indication of the complex non-linear mechanisms present in the vibration response of defective bearings.

4.2.1. IMF energy criterion

The energy of the n IMFs obtained using the EMD method is E_1, E_2, …, E_n. Table 2 shows the energy percent of the IMF components, which is designated as $P_i=E_i/E$, where E is the whole signal energy ($E=\Sigma_{i=1}^{n}E_i$ is equal to the total energy of the original signal due to the orthogonality of the EMD decomposition). The energy percentages of the first four IMF components are named as P_1, P_2, P_3 and P_4. P_5 is the energy percentage of the fifth IMF components and the remaining components (note that $P_5=(E_5+E_6+, \ldots,+E_n)/E$). From Table 2, we can see that the most dominant frequency and energy features of the outer race BD are mainly described by the first components. When the ORF occurs, the energy percentage of the first components will increase compared to healthy bearing.

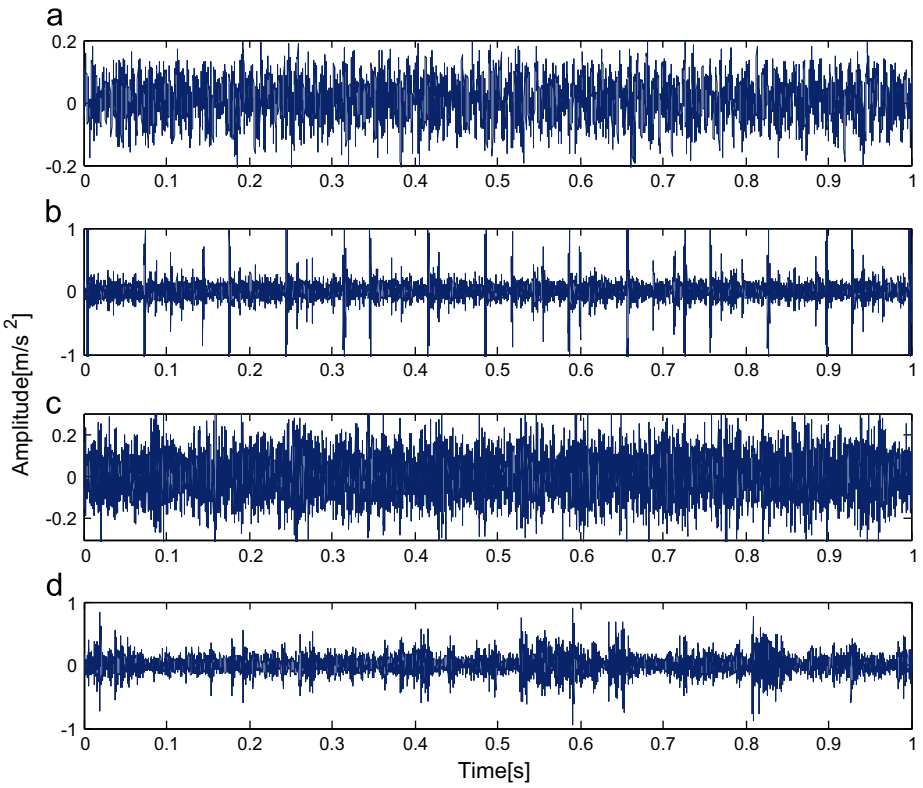

Fig. 9. An example of characteristics vibration signals under different bearing status at the same operating condition (1750 rpm speed and 1 hp load). (a) HB. (b) IRF; 0.1778 mm. (c) ORF; 0.1778 mm. (d) BF; 0.1778 mm.

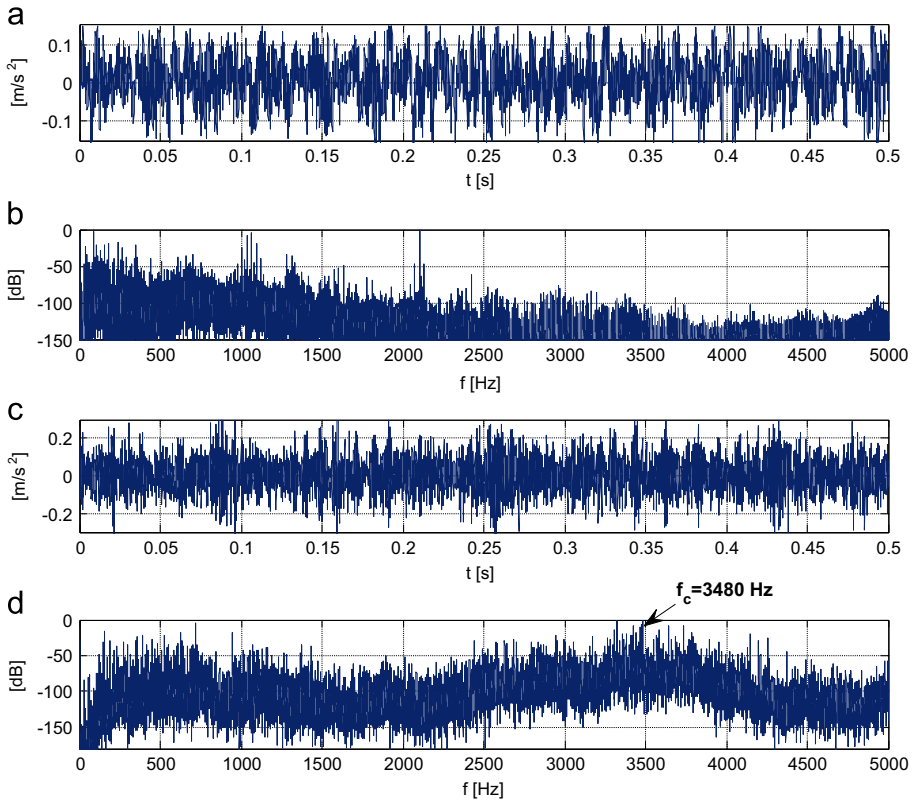

Fig. 10. An example of characteristics vibration signals under two different bearing status at the same operating condition (1750 rpm speed and 1 hp load). (a) Healthy bearing. (c) ORF; 0.1778 mm. (b) and (d) their PSD respectively.

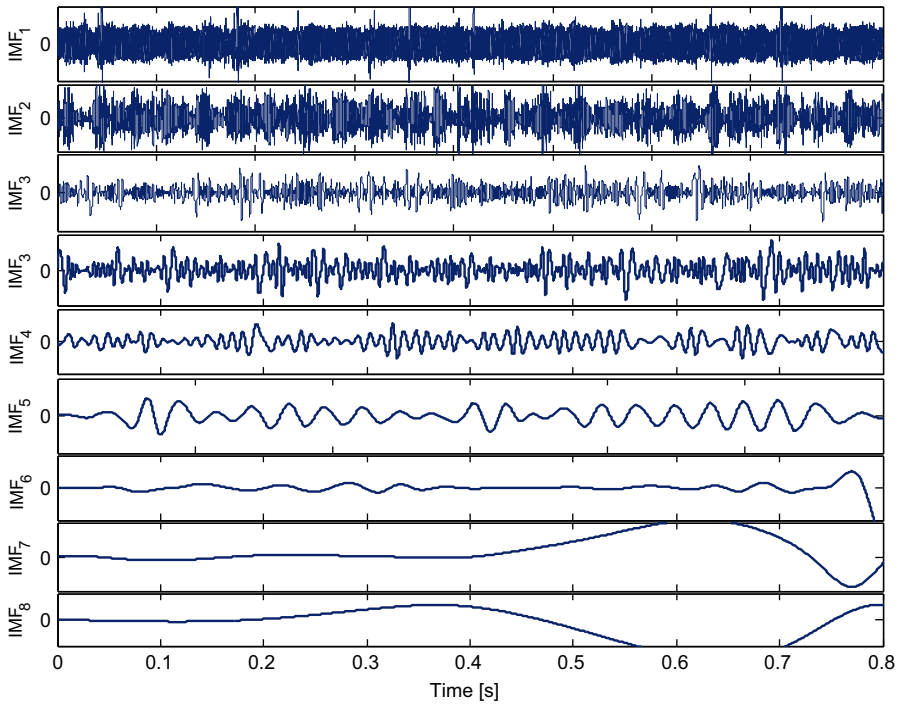

Fig. 11. First eight IMF components of healthy bearing vibration signal under the operating condition: 1750 rpm speed and 1 hp load.

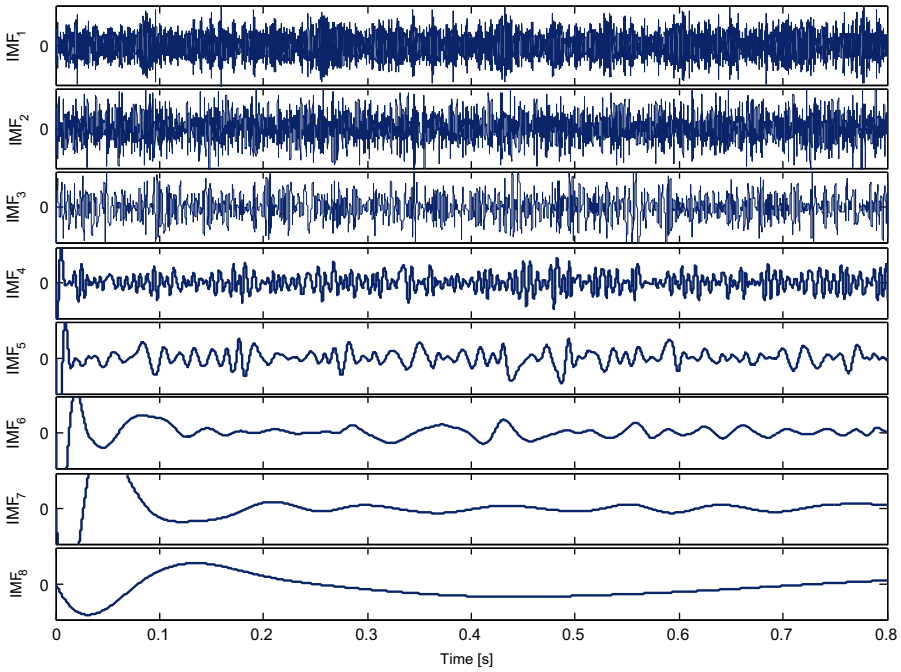

Fig. 12. First eight IMF components of the ORF bearing vibration signal under the operating condition: 1750 rpm speed and 1 hp load.

4.2.2. Statistical significance

The results shown in the paper seem to be from a single run of simulation/experiment. The results generated from the data do not have statistical significance and may not be able to generalize. A series of experiments should be conducted to support the author's claims. In addition, in fault detection problems, the performance of a detection algorithm usually depends on the trade-off between robustness and sensitivity. The sensitivity and robustness of the proposed BSEMD method need to be explored by running a series of experiments. A receiver operating characteristic (ROC) curve will make the results more convincing.

4.2.3. Detection performance evaluation: need for ROC analysis

To examine BSEMD detection measure's performance, ROC curves are often the only valid method of evaluation [26]. An ROC curves is a detection performance evaluation methodology, and demonstrates how effectively a certain detector can separate

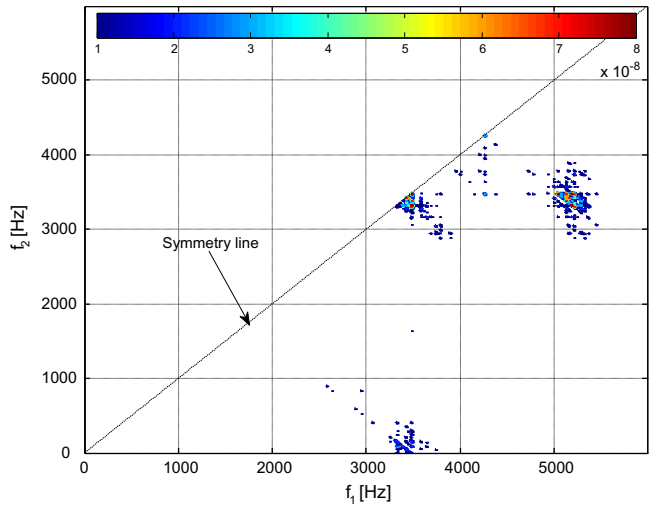

Fig. 13. Contour representation of the BSEMD of the first IMF-ORF bearing signal.

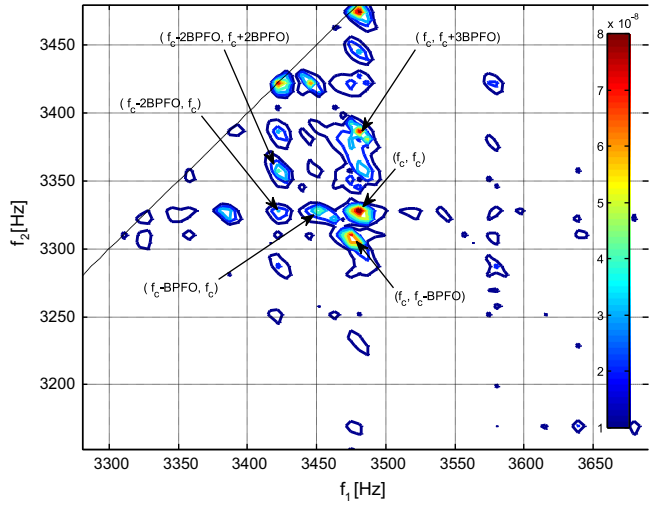

Fig. 14. Entire frequency band of Fig. 9, zoom in the area between 3200 and 3700 Hz in the f_1-f_2 spectral frequency axes.

two groups in a quantitative manner [26]. An ROC curve shows the trade-off between the probability of detection or true positives rate (*tpr*), also called sensitivity and recall versus the probability of false alarm or false positives rate (*fpr*). ROC curves are well described by Fawcett [26]. The *tpr* and *fpr* are mathematically expressed in (10) and (11), respectively.

$$tpr = \frac{true\ positives}{true\ positives + false\ negatives} \tag{10}$$

$$fpr = \frac{false\ positives}{false\ positives + true\ negatives} \tag{11}$$

For each case (Healthy, ORF, IRF and BF) and for each load and speed combinations ((0 hp, 1797 rpm), (1 hp, 1772 rpm), (2 hp, 1750 rpm), and (3 hp, 1730 rpm)), and under different BD severities (as shown in Table 3) a series of 70 independent Monte-Carlo experiments are conducted. For each experiment, the probability of false alarm and the probability of detection are obtained by counting detection results out of 3360 independent Monte-Carlo experiments by the BSEMD based method. The resultant ROC curve is shown in Fig. 15. Thus, when applied to experimental data from real bearings, the BSEMD method successfully identified

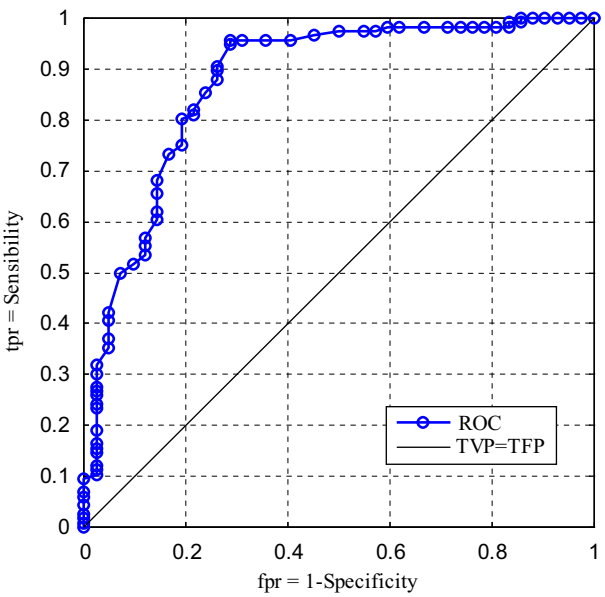

Fig. 15. ROC curve for BSEMD performance evaluation method.

more than 98.9% of the bearing data available with less than 1.1% error.

4.2.4. Discussion and comparison with some previous works

Table 4 provides a summary of the studies on identification of BDs. In conclusion, evaluation of our method versus previous researches given in Table 4, shows that our experiment demonstrates that BSEMD diagnosis scheme, containing non-stationary, non-Gaussian and non-linear information of the bearing vibration signal, and suggests that bi-spectrum combined with EMD has good potential for improving BDs diagnosis. BSEMD method produces a good performance measure: the accuracy result is 98.9%.

5. Discussion

This section summarizes the conclusions of the research performed and demonstrates the performance of BSEMD as a fault detection method. Future work is also proposed, suggesting application to other state-based data sources.

5.1. Conclusion

In order to make bearing fault diagnosis more convenient, accurate, and comprehensible, the advantages of the EMD method, and HOS are combined together to propose a new based approach called BSEMD. EMD is a self-adaptive signal processing method that can be used to preprocess the nonlinear and non-stationary signals perfectly. By analyzing of the outer race bearing signals from experiment rig, the results show that this method could identify the fault accurately and highlight the visibility of ORF signals. The BSEMD method is proved a promising way to fault diagnosing of rotating machinery. In addition, these results also show the advantages of the BSEMD method as applied to: noisy data, data which are unsuitable for frequency-domain analysis.

5.2. Future works

There are several possible directions for future Works based on this approach to fault detection. First, this work has application in fault detection for stochastic processes other than bearing fault data, and should be applied to detect multi-faults in induction

Table 4
Comparision of our proposed method with some previous work.

References	Methodologies	Performance measure
	Combinations of EMD with:	
Miao et al. [18]	Independent component analysis	– Its performance varies for different applications – Linear transformation
Yu et al. [19], Li et al. [20]	Teager Kaiser energy operator	– enhance the transient features and is suitable for detecting impact signals – calculated energy is derived from instantaneous amplitude and instantaneous frequency of the signal
Li and Zheng [22]	Wigner–Ville distribution	– High-load computation is needed – Resolution is not scalable
Li [21]	Order tracking	– Gives a calculation of the vibration signal sampled constant in angle from sampled constant in time. – High-load computation due to interpolation task
Chen et al. [23]	Wavelets	– Not easy to determine the optimal parameters for the wavelet filter – May compromise signal mathematical properties
Peng et al. [53]	Autoregressive model	– System model and measurement model need to be defined – Noise levels in both models could affect the performance and stability of the algorithm
Lei et al. [8]	Support vector machines	– No standard method to choose the kernel function which is the key process for SVM
Prposed method	Higher order statistics	– Sensitivity – 98.9% – Higher dimension system or more particles require too much computation cost – Filter out Gaussian noise – Nonlinearity detection in the signal

motor such as bearing and eccentricitie failures. This approach should be applied to other synthetic data sets and simulation models to further test its capacity for fault detection in clean or noisy data. Finally, this method stands to be implemented as a real-time fault detection metric in induction machine systems for active monitoring.

Acknowledgments

The authors wound like to thank the Case Western University Bearing Data Center for kindly providing the experimental data, analyzed in this paper, as well as we would like to thank Dr. Kenneth A. Loparo from the same University, for his experimental data provided.

References

[1] Seungdeog C, Akin B, Rahimian MM, Toliyat HA. Implementation of a fault-diagnosis algorithm for induction machines based on advanced digital-signal-processing techniques. IEEE Trans Ind Electron 2011;58(3):937–48.
[2] Saidi L, Henao H, Fnaiech F, Capolino G-A, Cirrincione G. Diagnosis of broken bars fault in induction machines using higher order spectral analysis. ISA Trans 2013;52:140–8.
[3] Randall RB, Antoni J. Rolling element bearing diagnostics – a tutorial. Mech Syst Signal Process 2011;25(2):485–520.
[4] Saidi L, Fnaiech F, Capolino G-A, Henao H. Stator current bi-spectrum patterns for induction machines multiple-faults detection. In: Proceedings of IEEE IECON; 2012. p. 5132–7.
[5] Montero FEH, Medina OC. The application of bispectrum on diagnosis of rolling element bearings: a theoretical approach. Mech Syst Signal Process 2008;22:588–96.
[6] Guoji S, McLaughlin S, Yongcheng X, White P. Theoretical and experimental analysis of bispectrum of vibration signals for fault diagnosis of gears. Mech Syst Signal Process 2014;43:76–89.
[7] Braun S, Feldman M. Decomposition of non-stationary signals into varying times scales: some aspects of the EMD and HVD methods. Mech Syst Signal Process 2011;25:2608–30.
[8] Lei Y, Lin J, He Z, Zuo MJ. A review on empirical mode decomposition in fault diagnosis of rotating machinery. Mech Syst Signal Process 2013;35:108–26.
[9] Flandrin P, Goncalvès P, Rilling G. Detrending and denoising with empirical mode decomposition. In: Proceedings of the 12th European signal processing conference; 2004. p. 1581–84.
[10] Mendel JM. Tutorial on higher order statistics (spectra) in signal processing and system theory: theoretical results and some applications. In: Proceedings of the IEEE, vol. 79; 1991. p. 287–05.
[11] Nikias CL, Petropulu A. Higher-order spectra analysis: a nonlinear signal processing framework. Englewood Cliffs, New Jersey: Prentice-Hall; 1993.
[12] Zhou Y, Chen J, Dong GM, Xiao WB, Wang ZY. Application of the horizontal slice of cyclic bispectrum in rolling element bearings diagnosis. Mech Syst Signal Process 2012;26:229–43.
[13] Saidi L., Henao H., Fnaiech F., Capolino G.-A., Cirrincione G. Application of higher order spectra analysis for rotor broken bar detection in induction machines. In: Proceedings of IEEE international symposium on diagnostics for electric machines power electronics & drives (SDEMPED); 2011. p. 31–8.
[14] Li H. Order bi-spectrum for bearing fault monitoring and diagnosis under run-up condition. J Comput 2011;6(9):1994–2000.
[15] Luo LJ, Yan Y, Xie P. Hilbert–Huang transform, Hurst and chaotic analysis based flow regime identification methods for an airlift reactor. Chem Eng J 2012;181–182:570–80.
[16] Tang J, Zhao LJ, Yue H. Vibration analysis based on empirical mode decomposition and partial least square. Proc Eng 2011;16:646–52.
[17] Lin JS, Chen Q. Application of the EEMD method to multiple faults diagnosis of gearbox. In: Proceedings of the second international conference on advanced computer control; 27–29, 2010. p. 395–9.
[18] Miao Q, Wang D, Pecht M. Rolling element bearing fault feature extraction using EMD-based independent component analysis. In: Proceedings of IEEE conference on prognostics and health management; 2011. p. 1–6.
[19] Yu DJ, Cheng JS, Yang Y. Application of EMD method and Hilbert spectrum to the fault diagnosis of roller bearings. Mech Syst Signal Process 2005;19:259–70.
[20] Li H, Zheng HQ. Bearing fault detection using envelope spectrum based on EMD and TKEO. In: Proceedings of the international conference on fuzzy systems and knowledge discovery; 2008. p. 142–6.
[21] Rai VK, Mohanty AR. Bearing fault diagnosis using FFT of intrinsic mode functions in Hilbert–Huang transform. Mech Syst Signal Process 2007;21:2607–15.
[22] Li H, Zheng HQ, Tang LW. Wigner–Ville distribution based on EMD for faults diagnosis of bearing. Fuzzy Syst Knowl Discov 2006;4223:803–12.
[23] Chen F., Zhou X., Wu Q.H. Application of Hilbert–Huang transformation to fault diagnosis of rotary machinery. In: Proceedings of International Symposium on Instrumentation Science and Technology; 2008. p. 15–8.
[24] Case Western Reserve University Bearing Data Center. Download a data file [DB/OL]. Available from: ⟨http://www.eecs.cast.edu/laboratory/bearing/download.htm⟩ (accessed 25.12.13).
[25] Priestley MB. Nonlinear and nonstationary time series analysis. NewYork: Academic Press; 1988.
[26] Fawcett T. An introduction to ROC analysis. Pattern Recognit Lett 2006;27:861–74.